American Mineralogist, Volume 97, pages 989–994, 2012

Tsilaisite, $NaMn_3Al_6(Si_6O_{18})(BO_3)_3(OH)_3OH$, a new mineral species of the tourmaline supergroup from Grotta d'Oggi, San Pietro in Campo, island of Elba, Italy

Ferdinando Bosi,[1,*] Henrik Skogby,[2] Giovanna Agrosì,[3] and Eugenio Scandale[3]

[1]Dipartimento di Scienze della Terra, Sapienza Università di Roma, P.le A. Moro, 5, I-00185 Rome, Italy
[2]Department of Mineralogy, Swedish Museum of Natural History, Box 50007, SE-10405 Stockholm, Sweden
[3]Dipartimento di Scienze della Terra e Geoambientali, Università di Bari, Campus, via E. Orabona 4, I-70125 Bari, Italy

Abstract

Tsilaisite, $NaMn_3Al_6(Si_6O_{18})(BO_3)_3(OH)_3OH$, is a long-expected new mineral of the tourmaline supergroup. It occurs in an aplitic dike of a LCT-type pegmatite body from Grotta d'Oggi, San Pietro in Campo, island of Elba, Italy, in association with quartz, K-feldspar, plagioclase, elbaite, and schorl. Crystals are greenish yellow with a vitreous luster, a white streak, and show no fluorescence. Tsilaisite has a Mohs hardness of approximately 7; it is brittle with a sub-conchoidal fracture, and has a calculated density of 3.133 g/cm^3. In plane-polarized light, tsilaisite is pleochroic, O = pale greenish yellow, E = very pale greenish yellow; it is uniaxial negative, $\omega = 1.645(5)$, $\varepsilon = 1.625(5)$. Tsilaisite is rhombohedral, space group *R*3*m*, $a = 15.9461(5)$, $c = 7.1380(3)$ Å, $V = 1571.9(1)$ Å^3, $Z = 3$. The strongest eight X-ray-diffraction lines in the powder pattern [*d* in Å(*I*)(*hkl*)] are: 3.974(100)(220), 2.942(94)(122), 2.570(79)(051), 2.034(49)(152), 4.205(41)(211), 6.329(22)(101), 2.377(21)(003), and 1.592(21)(550). Analysis by a combination of electron microprobe, secondary ion mass spectrometry, and optical absorption spectroscopy gives $SiO_2 = 36.10(3)$, $TiO_2 = 0.32(4)$, $Al_2O_3 = 37.10(5)$, MnO = 9.60(10), CaO = 0.09(4), $Na_2O = 2.11(7)$, $K_2O = 0.03(1)$, F = 0.79(3), $B_2O_3 = 10.2(6)$, $Li_2O = 0.8(1)$, $H_2O = 3.1(2)$, sum 99.95 wt%. The unit formula is $^{X}(Na_{0.67}\square_{0.30}Ca_{0.02}K_{0.01})^{Y}(Mn^{2+}_{1.34}Al_{1.14}Li_{0.54}Ti_{0.04})^{Z}Al_6{}^{T}(Si_{5.94}Al_{0.06})B_{2.91}O_{27}{}^{V}(OH)_3{}^{W}(OH_{0.39}F_{0.41}O_{0.20})$. The structure, refined also taking into account the positional disorder of the O1 and O2 anions, converged to statistical indices *R*1 for all reflections of about 2%. The resulting site populations indicate that the Z site is occupied by Al and that the Y site is dominated by Mn^{2+}. Aluminum is incorporated at Y through two types of substitutions: $^{Y}Al+{}^{W}O^{2-} \rightarrow {}^{Y}Mn^{2+}+{}^{W}OH$, which has the result of replacing OH at the W site by O^{2-}, and $^{Y}(Al+Li)+{}^{W}F \rightarrow 2{}^{Y}Mn^{2+}+{}^{W}OH$, which relates fluor-elbaite to the tsilaisite component. Infrared absorption spectra measured in the principal OH-stretching region were interpreted on the basis of local arrangements consistent with the short-range bond-valence requirements. A compositional trend from fluor-elbaite to tsilaisite is observed in samples from Elba Island. The occurrence of tsilaisite is very rare in nature, as a consequence of both the requirement of extraordinary petrogenetic conditions and limited structural stability.

Keywords: Tsilaisite, tourmaline, new mineral species, crystal-structure refinement

Introduction

The tourmaline supergroup minerals occur typically as accessory phases (but occasionally as minor or even major minerals) in a wide range of rocks of variable origin and composition, including granitic pegmatites. They are known as valuable indicator minerals that can provide information on the compositional evolution of their host rocks, chiefly due to their ability to incorporate a large number of elements (e.g., Novák et al. 2004, 2011; Agrosì et al. 2006; Lussier et al. 2011a; van Hinsberg et al. 2011). However, the chemical composition of tourmalines is also strongly controlled by various crystal-structural constraints (e.g., Hawthorne 1996, 2002; Bosi 2010, 2011). The crystal structure and crystal chemistry of tourmaline have been extensively studied (e.g., Foit 1989; Hawthorne 1996; Hawthorne and Henry 1999; Bosi and Lucchesi 2007; Bosi 2008; Lussier et al. 2008, 2011b; van Hinsberg and Schumacher 2009; Bosi et al. 2010). The general formula of tourmaline may be formalized as: $XY_3Z_6T_6O_{18}(BO_3)_3V_3W$, where $^{[9]}X$ = Na, Ca, □ (=vacancy), K; $^{[6]}Y$ = Al, Fe^{3+}, Cr^{3+}, V^{3+}, Mg, Fe^{2+}, Mn^{2+}, Li, Ti^{4+}; $^{[6]}Z$ = Al, Fe^{3+}, Cr^{3+}, V^{3+}, Mg, Fe^{2+}; $^{[4]}T$ = Si, Al, B; $^{[3]}B$ = B; $^{[3]}V(\equiv O3)$ = OH, O; $^{[3]}W(\equiv O1)$ = OH, F, O. The dominance of these ions at one or more sites of the structure gives rise to many distinct mineral species (Henry et al. 2011).

In this paper, we describe the long-expected new mineral tsilaisite, from Grotta d'Oggi, San Pietro in Campo, Elba, Italy. In his work on tourmaline chemistry, Kunitz (1929) proposed the name tsilaisite for a hypothetical tourmaline end-member characterized by the presence of Na, Mn^{2+}, and Al. The name, originally used to designate yellow tourmalines, was derived from the Tsilaisina mine in the Sahatany Valley (Madagascar) where the first Mn-rich tourmalines were found and described by Duparc et al. (1910), and recently also by Simmons et al. (2011). Nuber and Schmetzer (1984) reported the first crystal structure of a tourmaline with MnO contents of 6.72 wt%, while Burns et al. (1994) demonstrated the occurrence of positional disorder at the O1 and O2 anion sites in tourmalines with MnO contents ranging

* E-mail: ferdinando.bosi@uniroma1.it

0003-004X/12/0506–989$05.00/DOI: http://dx.doi.org/10.2138/am.2012.4019

from 0.35 to 6.23 wt%. Although in gemology the tsilaisite term has always been used to refer to a yellow specimen without a brown cast and the tsilaisite component has often been identified in several tourmalines from different localities (e.g., Simmons et al. 2011 and references therein), the existence of a sample with an appropriate composition was never found in nature and the true tsilaisite has been expected for about a century. The ideal formula of tsilaisite as well as relevant substitution mechanisms have been a matter of discussion in the literature; e.g., Slivko (1959, 1961) suggested the formula $Na(MnAl_2)Al_6(Si_6O_{18})(BO_3)_3[(OH)_2O]O$; Schmetzer and Bank (1984) suggested $Na(Mn_{1.5}Al_{1.5})Al_6(Si_6O_{18})(BO_3)_3O_{1.5}(OH,F)_{2.5}$ and related to elbaite by the substitution $Li+OH \rightarrow Mn^{2+}+O^{2-}$; London (2011) suggested $Na(LiMnAl)Al_6(Si_6O_{18})(BO_3)_3(OH)_4$, this being related to schorl by the substitution $3Fe^{2+} \rightarrow (Li+Mn^{2+}+Al)$. Other possible end-member formulas and relationships to other species of Mn^{2+}-rich tourmalines are discussed in Hawthorne and Henry (1999). Just after the publication of the revised tourmaline nomenclature (Henry et al. 2011), we realized that the composition of sample Tsl2g reported in Bosi et al. (2005a) is consistent with the end-member proposed by Kunitz (1929): $NaMn_3Al_6(Si_6O_{18})(BO_3)_3(OH)_3OH$.

The new mineral and its name have since been approved by the International Mineralogical Association Commission on New Minerals, Nomenclature and Classification (IMA 2011-047). The holotype specimen of tsilaisite is deposited in the collections of the Museo di Scienze della Terra, settore Mineralogico Petrografico "Carlo Lorenzo Garavelli," Campus Universitario, Bari, Italy (sample 12/nm).

Occurrence, appearance, physical and optical properties

Tsilaisite occurs in an aplitic dike of an LCT-type pegmatite body at Grotta d'Oggi, San Pietro in Campo, Elba, Italy (Bosi et al. 2005a; Agrosì et al. 2006), in association with quartz, K-feldspar, plagioclase, elbaite, and schorl. Tsilaisite is greenish yellow with a vitreous luster. It has a white streak and shows no fluorescence. The samples appear frequently as color-zoned tsilaisite-elbaite crystals of about 6 to 9 mm in length and 16 to 60 mm^2 in basal section. Their morphology consists of elongated $\{10\bar{1}0\}$ and $\{11\bar{2}0\}$ prisms terminated by a prominent {0001} pedion and small, minor $\{10\bar{1}1\}$ pyramidal faces. Prism faces are striated (Fig. 1). Tsilaisite has a Mohs hardness of approximately 7 and is brittle with a $\{10\bar{1}1\}$ and $\{11\bar{2}0\}$ imperfect cleavage, {0001} parting and sub-conchoidal fracture. The calculated density is 3.133 g/cm^3. In transmitted light, tsilaisite is pleochroic with O = pale greenish yellow and E = very pale greenish yellow. Tsilaisite is uniaxial negative with refractive indices, measured by the immersion method using white light from a tungsten source, of $\omega = 1.645(5)$, $\varepsilon = 1.625(5)$. The mean index of refraction, density, and chemical composition lead to an excellent compatibility index ($1 - K_p/K_c = 0.035$) (Mandarino 1976, 1981).

Methods

Chemical data

The composition of the tsilaisite sample Tsl2g has already been reported in Bosi et al. (2005a). These authors studied the crystal chemistry of seven crystal fragments taken from different regions of the same tourmaline crystal (see Fig. 1 of Bosi et al. 2005a). The tsilaisite sample Tsl2g is one of these fragments, which was situated at the center of the more strongly colored basal region of the crystal. In detail, 10 chemical spot analyses on sample Tsl2g were carried out using an electron microprobe in WDS mode. Ion microprobe (secondary ion mass spectrometry) was also used for H_2O, Li_2O, and B_2O_3 measurements. Analytical data are given in Table 1.

To determine the valence state of manganese that may be present in the form of Mn^{2+} and Mn^{3+}, we measured optical absorption spectra polarized in the ε and ω directions on a 330 μm thick crystal section. The acquired spectra are very similar to those obtained on Mn-rich elbaite by Rossman and Mattson (1986), with a weak band at 635 nm assigned to Mn^{2+}; no bands that could be assigned to absorption by Mn^{3+} were detected. Since Mn^{3+} bands are expected to have a considerably higher molar absorptivity than Mn^{2+} bands (e.g., Bosi et al. 2007), we conclude that Mn occurs only in the divalent state in the present sample.

As Rossman and Mattson (1986) concluded based on optical absorption spectra of a series of Mn-bearing elbaite crystals, the green-yellow color of the tsilaisite (Tsl2g) can also be ascribed to Mn^{2+}-Ti^{4+} intervalence charge transfer interaction, which absorbs the violet to blue portion of the visible spectrum. Although the Mn content of the Tsl2g sample is higher compared to the previously studied Mn-bearing elbaite samples, the Ti content is very similar (0.3 wt% TiO_2).

X-ray powder diffraction

The powder-diffraction pattern was collected using a Philips PW1050 diffractometer with a graphite monochromatized Cu*K* (λ = 1.54056 Å) radiation. Extracted *d* values are listed in Table 2. Unit-cell parameters from the powder data were refined using the Rietveld method.

Single-crystal structural refinement

Details of single-crystal X-ray data collection are reported in Bosi et al. (2005a). However, that structure refinement was not performed in a completely optimal way and may involve errors due to the use of a very high resolution (d_{min} = 0.48 Å), which may introduce errors due to biased data, lack of evaluation of merohedral/racemic twins by the Flack parameter, and the use of an inappropriate weighting scheme as indicated by the goodness-of-fit = 1.401. Furthermore, additional information such as

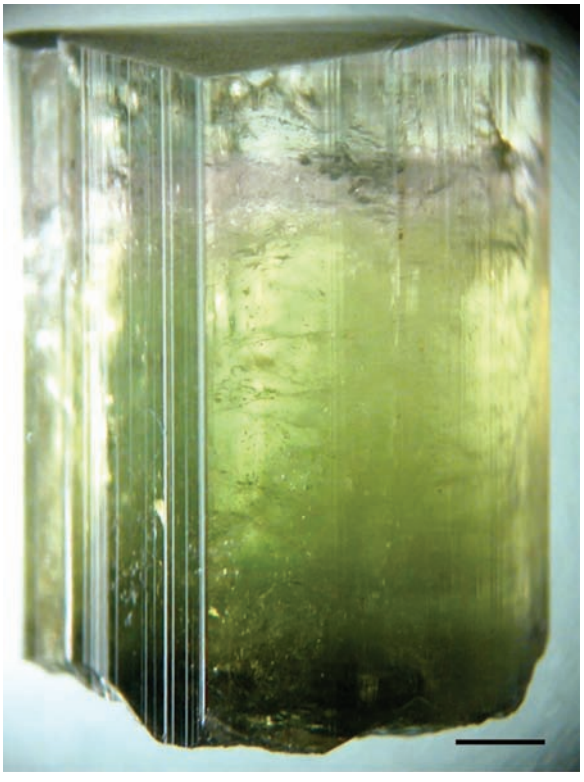

Figure 1. Crystal of color-zoned tourmaline from Grotta d'Oggi, island of Elba, Italy. Bar = 1 mm. The Tsl2g fragment was extracted from the center of the basal region of the crystal. (Color online.)

TABLE 1. Chemical composition and atomic proportions of tsilaisite

Sample	Tsl2g					
Number of points	10				Atomic proportions	
	Mean	Range	Stand. Unc.	Probe standard		
SiO_2 wt%	36.10	35.90–36.50	0.30	Wollastonite	Si apfu	5.94(7)
TiO_2	0.32	0.28–0.35	0.04	Rutile	Ti^{4+}	0.04(1)
B_2O_3	10.24	9.96–10.67	0.56	Elbaite	B	2.91(14)
Al_2O_3	37.10	36.70–37.80	0.05	Jadeite	Al	7.20(6)
MnO	9.60	9.50–9.80	0.10	Rhodonite	Mn^{2+}	1.34(2)
FeO	n.d.	–	–	Magnetite	–	–
MgO	n.d.	–	–	Periclase	–	–
ZnO	n.d.	–	–	Metallic Zn	–	–
CaO	0.09	0.05–0.14	0.04	Wollastonite	Ca	0.02(1)
Na_2O	2.11	2.01–2.19	0.07	Jadeite	Na	0.67(2)
K_2O	0.03	0.02–0.04	0.01	Orthoclase	K	0.007(2)
Li_2O	0.81	0.76–0.85	0.10	Elbaite	Li	0.54(7)
F	0.79	0.75–0.82	0.03	F-phlogopite	F	0.41(2)
H_2O	3.09	3.01–3.31	0.16	Elbaite	OH	3.39(17)
–O=F	–0.33					
Total	99.95					

Notes: Atomic proportions normalized to 31 anions. Standard uncertainties for the atomic proportions (in parentheses) were calculated by error propagation. n.d. = not detected.

TABLE 2. X-ray powder diffraction data for tsilaisite

I	d_{meas} (Å)	d_{calc} (Å)	*h k l*
22	6.33(2)	6.337	1 0 1
19	4.95(1)	4.958	0 2 1
7	4.595(9)	4.597	0 3 0
41	4.205(8)	4.209	2 1 1
100	3.974(7)	3.981	2 2 0
71	3.452(5)	3.454	0 1 2
14	3.367(5)	3.371	1 3 1
7	3.008(4)	3.009	4 1 0
94	2.942(4)	2.944	1 2 2
9	2.889(4)	2.892	3 2 1
5	2.607(3)	2.609	3 1 2
79	2.570(3)	2.573	0 5 1
21	2.377(2)	2.378	0 0 3
10	2.338(2)	2.340	5 1 1
9	2.181(2)	2.182	5 0 2
19	2.159(2)	2.161	4 3 1
14	2.110(2)	2.112	0 3 3
16	2.041(2)	2.042	2 2 3
49	2.034(2)	2.035	1 5 2
7	2.016(2)	2.017	1 6 1
18	1.907(8)	1.913	3 4 2
5	1.768(1)	1.769	1 0 4
18	1.652(1)	1.653	0 6 3
21	1.592(1)	1.592	5 5 0
5	1.582(1)	1.582	4 5 2
19	1.497(1)	1.498	0 5 4
15	1.446(1)	1.446	6 4 2
10	1.401(1)	1.402	4 3 4

Notes: I = measured intensity, d_{meas} = measured interplanar spacing; d_{calc} = calculated interplanar spacing; *hkl* = reflection indices. Estimated standard uncertainty in parentheses. Unit-cell parameters: $a = 15.922(1)$, $c = 7.133(1)$ Å, $V = 1566.0(2)$ Å^3.

the positional disorder of the O1 and O2 anions in the crystal structure can be obtained from that data set. Consequently, a new structural refinement has been carried out, with the SHELXL program (Sheldrick 2008), applying a resolution cut-off at $d_{min} = 0.62$ Å, determining the Flack parameter, using the weighting scheme suggested by SHELXL, allowing disordering of O1 and O2 in accord with the recommendations of Burns et al. (1994) and modeling the T and B sites with fixed occupancy of 1 since no significant deviations occurred from this value. No correlations over 0.7 between the parameters were observed at the end of refinements.

This critical examination led to better statistical factors and confirmed the correctness of the structural parameters reported by Bosi et al. (2005a), showing that the improved new values for these parameters do not differ significantly from the original ones. Statistical details are given in Table 3[1]; atom coordinates and equivalent displacement parameters are in Table 4[1]; anisotropic displacement parameters are in Table 5[1]; bond lengths and mean atomic numbers (m.a.n) are in Table 6[1].

Finally, it should be noted that two important findings arise from this new structural re-examination. First, the simultaneous refinement of a large portion of the total scattering is possible in the tourmaline structure, because it may or may not yield correlations between site occupancy and scale factor. In fact, very similar results were obtained when simultaneously refining the occupancy of all cation sites (X, Y, Z, T, B) , as was done by Bosi et al. (2005a), or when constraining the site occupancy of T and B to 1. Second, the Z-site scattering refinement (m.a.n. = 13.2) supports the presence of small amounts of Mn^{2+} at this site, which is not in conflict with either short-range bond-valence constraints at the O1 and O3 sites (e.g., Hawthorne 1996; Bosi 2011) or the partition coefficients calculated for Mn^{2+} by the lattice-strain theory (van Hinsberg 2011).

Infrared spectroscopy

Polarized FTIR absorption spectra in the wavenumber range of 2000–5000 cm^{-1} were collected on a tsilaisite single-crystal section orientated parallel to the **c**-axis direction using a Bruker Equinox 55 spectrometer equipped with a NIR source, a CaF_2 beam-splitter, and an InSb detector. A circular aperture with a diameter of 400 µm was used to mask the IR beam on the 31 µm thick crystal. A total of at least 200 scans in dry air were performed for each measurement (parallel and perpendicular to the crystallographic **c**-axis) and background with a resolution of 4 cm^{-1}.

RESULTS AND DISCUSSION

Mineral chemistry

In accordance with the classification procedure of Henry et al. (2011) the empirical ordered formula of tsilaisite sample Tsl2g (Table 1) can be written as

$$^{X}(Na_{0.67}\square_{0.30}Ca_{0.02}K_{0.01})^{Y}(Mn^{2+}_{1.34}Al_{1.14}Li_{0.54}Ti_{0.04})^{Z}Al_6{}^{T}(Si_{5.94}Al_{0.06})B_{2.91}O_{27}{}^{V}(OH)_3{}^{W}(OH_{0.39}F_{0.41}O_{0.20}).$$

This ordered formula is consistent with a ^{Z}Al-dominant tourmaline belonging to the alkali group-subgroup 1: Na-dominant at the X position and OH+F > O^{2-} at the W position of the general formula. As the content of Mn^{2+} is larger than that of 2Li at the Y position (1.34 and 1.08 apfu, respectively) and because no tourmalines have yet been documented as $^{Y}Mn^{2+}$-dominant, this tourmaline can be classified as a new species (Fig. 2). To assign a correct name, we had to determine if this $^{Y}Mn^{2+}$-dominant tour-

[1] Deposit item AM-12-038, Tables 3–6 and CIFs. Deposit items are available two ways: For a paper copy contact the Business Office of the Mineralogical Society of America (see inside front cover of recent issue) for price information. For an electronic copy visit the MSA web site at http://www.minsocam.org, go to the *American Mineralogist* Contents, find the table of contents for the specific volume/issue wanted, and then click on the deposit link there.

maline belongs to the hydroxy or fluor subgroup. To do this, the occupancy of the W position needed to be scrutinized as the OH and F contents are statistically equal, being 0.39 ± 0.17 and 0.41 ± 0.02, respectively. Of particular interest in this regard is the occurrence of O^{2-} at the W position in the formula, which may be related to either the substitution $^{Y}Al+^{W}O^{2-} \rightarrow {}^{Y}Mn^{2+}+{}^{W}OH$ or $^{Y}Al+^{W}O^{2-} \rightarrow {}^{Y}Mn^{2+}+{}^{W}F$. However, from the inverse correlation between Mn^{2+} and F ($r^2 = 0.86$) observed in Mn-rich tourmaline fragments from the same macro-crystal (Bosi et al. 2005a), it is clear that as Mn^{2+} contents increase there is a concomitant decrease in F towards the composition of the tsilaisite end-member. Such a trend is also confirmed in other Mn-,F-bearing elbaite and fluor-elbaite samples (Fig. 3), although the incorporation of F in tourmaline is affected by other factors such as local X- and Y-site charge (Henry and Dutrow 2011). As a result, the occurrence of $^{W}O^{2-}$ is related to $^{Y}Al+^{W}O^{2-} \rightarrow {}^{Y}Mn^{2+}+{}^{W}OH$. Through this substitution, $^{W}O^{2-}$ is replaced by ^{W}OH (and ^{Y}Al by $^{Y}Mn^{2+}$) giving the composition $^{X}(Na_{0.7}\square_{0.3})^{Y}(Mn_{1.5}Al_{0.9}Li_{0.5})^{Z}(Al_6)(Si_6O_{18})(BO_3)_3(OH)_3{}^{W}(OH_{0.6}F_{0.4})$ that belongs to the hydroxyl subgroup with $^{W}OH > {}^{W}F$. As a result, the correct name is tsilaisite, without any "fluor-" prefix modifier. In addition, it should be noted that as the uncertainty associated with measuring OH is relatively large compared to that of F, the latter could be recommended as a prefix only in cases where the criterion F > 0.5 atoms per formula unit (apfu) is fulfilled.

In general, minor constituents are related to the following additional substitutions in the tsilaisite sample Tsl2g

$^{Y}Mn^{2+}+{}^{W}OH \leftrightarrow {}^{Y}Al+{}^{W}O^{2-}$, which relates to deprotonization (1)

$^{X}Na+{}^{Y}Mn^{2+} \leftrightarrow {}^{X}\square+{}^{Y}Al$, which relates to alkali vacancy (2)

$2{}^{Y}Mn^{2+}+{}^{W}OH \leftrightarrow {}^{Y}(Al+Li)+{}^{W}F$, which relates to the fluor-elbaite component (3)

$2{}^{Y}Mn^{2+} \leftrightarrow {}^{Y}(Al+Li)$, which relates to the elbaite component. (4)

Through these substitutions the tsilaisite end-member composition can be easily achieved from the Tsl2g sample: substitutions 1 and 2 lead to $^{X}(Na)^{Y}(Mn_{1.8}Al_{0.6}Li_{0.5})^{Z}(Al_6)(Si_6O_{18})(BO_3)_3(OH)_3{}^{W}(OH_{0.6}F_{0.4})$; substitutions 3 and 4 lead to $NaMn_3Al_6(Si_6O_{18})(BO_3)_3(OH)_3OH$, within analytical uncertainty.

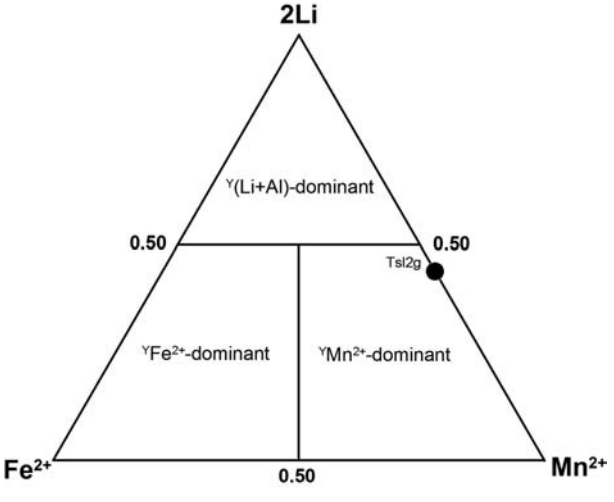

FIGURE 2. Ternary diagram for 2Li-Fe^{2+}-Mn^{2+} subsystem used for illustrating the dominant occupancy of the Y site for tourmaline.

Short-range arrangements

In theory, 30 short-range W-site arrangements compatible with the chemical composition of the tsilaisite sample Tsl2g are possible: ^{Y}(LiLiAl)–^{W}(OH,F,O^{2-}); ^{Y}(MnMnMn)–(OH,F,O^{2-}); ^{Y}(LiMnAl)–(OH,F,O^{2-}); ^{Y}(LiMnMn)–(OH,F,O^{2-}); ^{Y}(LiAlAl)–(OH,F,O^{2-}); ^{Y}(MnMnAl)–(OH,F,O^{2-}); ^{Y}(LiLiLi)–(OH,F,O^{2-}); ^{Y}(AlAlAl)–(OH,F,O^{2-}); ^{Y}(LiLiMn)–(OH,F,O^{2-}); ^{Y}(MnAlAl)–(OH,F,O^{2-}), where (OH,F,O^{2-}) correspond to three different W-site arrangements. However, this number can be reduced by applying bond-valence theory to the questions of local arrangements. Results of this approach showed that short-range bond-valence requirements around the W site of tourmaline exert strong constraints on the local arrangements of atoms that can occur (Hawthorne 1996, 2002; Bosi 2010, 2011). Consequently, the number of arrangements that are stable can be reduced to 14: ^{Y}(LiMnAl)–^{W}(OH,F); ^{Y}(MnMnMn)–^{W}(OH,F); ^{Y}(MnMnAl)–^{W}(OH,F); ^{Y}(LiAlAl)– ^{W}(OH,F); ^{Y}(LiLiAl)–^{W}(OH,F); ^{Y}(LiMnMn)–^{W}(OH,F); ^{Y}(AlAlAl)–^{W}(O^{2-}); ^{Y}(MnAlAl)–^{W}(O^{2-}).

Among these 14 local arrangements, only 6 may give rise to the OH-stretching absorption at the W site, since arrangements involving ^{W}F and $^{W}O^{2-}$ obviously do not give rise to any OH-stretching absorption.

Local arrangement around OH groups

Each of the local arrangements around the two types of OH groups, which occupy two different crystallographic sites (O1≡W and O3≡V), is expected to produce an absorption band in the infrared spectrum. The W site is surrounded by 3Y cations, whereas

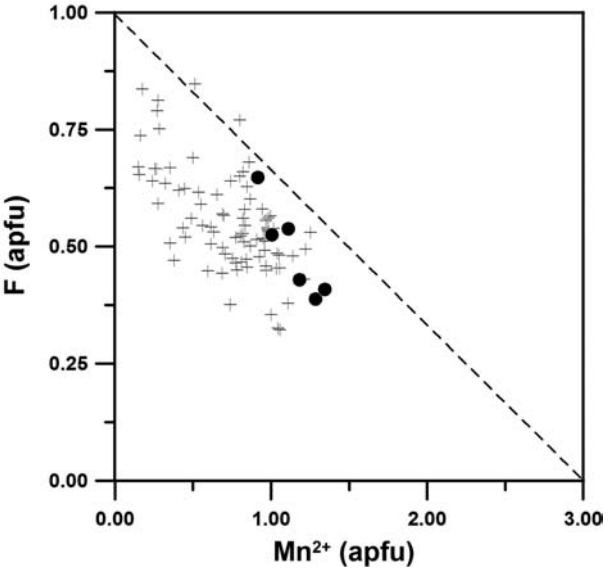

FIGURE 3. Plot of F content against Mn^{2+} content in Mn-,F-bearing elbaite, fluor-elbaite, and tsilaisite samples with Mn^{2+} and F > 0.15 apfu and Fe^{2+} < 0.5 apfu showing that such an inverse correlation implies a F-poor Mn end-member. Black circles: Bosi et al. (2005a); black crosses: Sahama et al. (1979), Schmetzer and Bank (1984), Shigley et al. (1986), Burns et al. (1994), Federico et al. (1998), Ertl et al. (2003), Bosi et al. (2005b), Lussier et al. (2009), Shabaga et al. (2010), Ertl et al. (2010), Simmons et al. (2011), Bosi (unpublished Mn-bearing fluor-elbaite).

the V site is surrounded by Y+2Z cations. Spectra recorded in polarized mode perpendicular and parallel to the crystallographic **c**-axis show several absorption bands within the 3800 to 3300 cm^{-1} spectral region (Fig. 4). In tourmaline minerals, OH absorption bands polarized parallel to the crystallographic **c**-axis direction are extremely intense, and it is notoriously difficult to prepare sections thin enough to avoid saturation effects, which are evident for the strongest bands in the present spectra. The spectral interpretation was therefore based also on data obtained from the direction perpendicular to the **c**-axis. The assignment of OH absorption bands in infrared spectra to specific local cation arrangements has been addressed in several previous studies, however, the proposed assignment models are generally not in agreement (e.g., Gonzalez-Carreño et al. 1988; Castañeda et al. 2000). In line with other studies, including other mineral groups (e.g., Martìnez-Alonso et al. 2002), we assume that the frequency of observed absorption bands is inversely related to the sum of charges of cations, which are coordinated to the OH group. We also assume that the ^{W}OH group is an independent entity in the structure (i.e., no or very weak hydrogen bond may occur), whereas the ^{V}OH group forms hydrogen bond with the closest O5 atom (^{V}O–H···O5). This latter assumption implies that the bond valence incident at W is lower than that incident at V, about 1.05 and 1.15 v.u., respectively. On these bases, an assignment model of the fitted bands to the stable short-range arrangements is proposed as follows: the occurrence of bands at wavenumbers larger than 3600 cm^{-1} are assigned to ^{W}OH, bands in the region 3600–3400 cm^{-1} are assigned to ^{V}OH and the band at about 3350 cm^{-1} is due to the hydrogen bond ^{V}O–H···O5. More details are reported in Table 7. Note that the local arrangements assigned to bands related to ^{V}OH and the band at 3672 cm^{-1} related to ^{W}OH are consistent with the assignments of Gonzalez-Carreño et al. (1988).

Relations to other species

Simmons et al. (2011) showed that Mn-rich yellow to yellow-greenish tourmalines are predominantly Mn^{2+}-rich (>3 wt% MnO) elbaite and fluor-elbaite (IMA 2011-071, Bosi et al. 2011), and suggested the occurrence of a solid solution between elbaite and the hypothetical tsilaisite. To demonstrate the validity of such a conclusion, we use the series of seven tourmalines reported in Bosi et al. (2005a). These samples can be classified as fluor-elbaite, Mn^{2+}-rich fluor-elbaite, and tsilaisite. Figure 5 clearly shows that there is an evolution from fluor-elbaite to tsilaisite in accord with the substitutions 3 and 4.

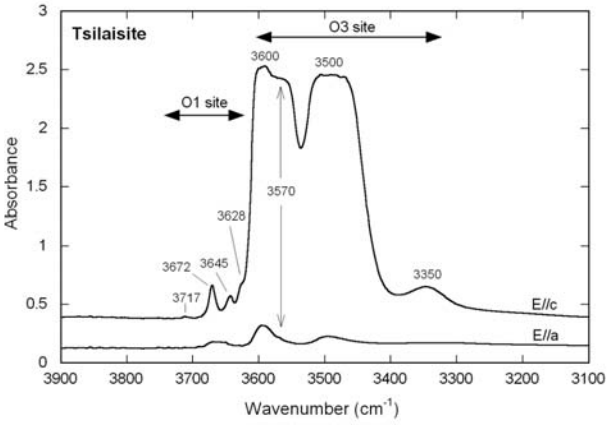

FIGURE 4. Polarized FTIR absorption spectra in the OH-stretching frequency region of tsilaisite. The spectra were measured on a 31 µm thick crystal section and are vertically offset for clarity.

Occurrence and stability of tsilaisite

Simmons et al. (2011) suggested that the formation of yellow tourmalines in nature, and then tsilaisite, requires very specific conditions: the original pegmatite-forming melt (preferably a B-rich peraluminous melt) must be relatively low in Fe and enriched in Mn and B, moreover, during the early stages of crystallization Fe must be removed, but abundant B and Mn must still be available when tourmaline crystallizes. Beside these peculiar petrogenetic conditions, we should also consider the failure to synthesize the tsilaisite end-member (e.g., Choi and Grover 2006; London 2011 and references therein), with the highest amounts of Mn incorporated into synthetic tourmaline structure being around 1.5 apfu. These observations are in line with the predictions by Bosi and Lucchesi (2007), who attributed the limitation in accommodating $^{Y}Mn^{2+}$ in tourmaline to a dimensional misfit between YO_6 and ZO_6. Because of this

TABLE 7. Local arrangements related to the fitted absorption bands in IR spectra of tsilaisite

Band	Local arrangement
~3350 cm^{-1}	O3–H···O5 (hydrogen bond)
~3500	$(^{Y}Al\ ^{Z}Al\ ^{Z}Al)^{9+}$–O3
~3570	$(^{Y}Mn\ ^{Z}Al\ ^{Z}Al)^{8+}$–O3
~3600	$(^{Y}Li\ ^{Z}Al\ ^{Z}Al)^{7+}$–O3
~3628	$^{Y}(Mn\ Mn\ Al)^{7+}$ or $^{Y}(Li\ Al\ Al)^{7+}$–O1
~3645	$^{Y}(Mn\ Mn\ Al)^{7+}$, $^{Y}(Li\ Al\ Al)^{7+}$ or $^{Y}(Mn\ Mn\ Mn)^{6+}$–O1
~3672	$^{Y}(Li\ Mn\ Al)^{6+}$–O1
~3717	$^{Y}(Li\ Mn\ Mn)^{5+}$ or $^{Y}(Li\ Li\ Al)^{5+}$–O1

Note: O1≡^{W}OH; O3≡^{V}OH.

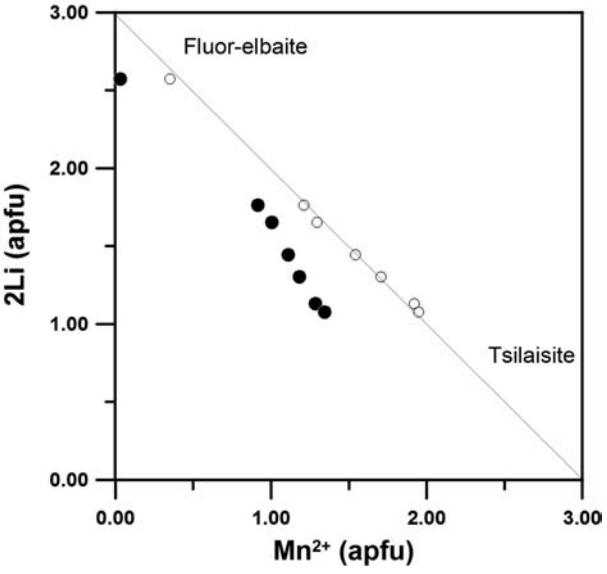

FIGURE 5. Plot of 2Li content against Mn^{2+} content showing the evolution from fluor-elbaite to tsilaisite in tourmalines from Elba Island. Black circles: observed composition; white circles: calculated composition via the substitutions 1 and 2 (see text), which result in replacement of $^{Y}Al_{excess}$ (=$^{Y}Al_{total}$ – Li) by $^{Y}Mn^{2+}$.

geometrical constraint, a concentration of $^{Y}Mn^{2+} > 1.5$ apfu may lead to structural instability. All these studies converge to the final conclusion that the occurrence of tsilaisite composition approaching the end-member is very rare in nature, as a consequence of both the requirement of extraordinary petrogenetic conditions and limited structural stability.

ACKNOWLEDGMENTS

We thank U. Hålenius for his kind assistance in the collection and interpretation of optical absorption spectra, and P. Ballirano for the Rietveld calculation. We also thank the AE F. Colombo, B. Dutrow, and an anonymous reviewer for their useful suggestions.

REFERENCES CITED

Agrosì, G., Bosi, F., Lucchesi, S., Melchiorre, G., and Scandale, E. (2006) Mn-tourmaline crystals from island of Elba (Italy): Growth history and growth marks. American Mineralogist, 91, 944–952.

Bosi, F. (2008) Disordering of Fe^{2+} over octahedrally coordinated sites of tourmaline. American Mineralogist, 93, 1647–1653.

——— (2010) Octahedrally coordinated vacancies in tourmaline: a theoretical approach. Mineralogical Magazine, 74, 1037–1044.

——— (2011) Stereochemical constraints in tourmaline: from a short-range to a long-range structure. Canadian Mineralogist, 49, 17–27.

Bosi, F. and Lucchesi, S. (2007) Crystal chemical relationships in the tourmaline group: structural constraints on chemical variability. American Mineralogist, 92, 1054–1063.

Bosi, F., Hålenius, U., Andreozzi, G.B., Skogby, H., and Lucchesi, S. (2007) Structural refinement and crystal chemistry of Mn-doped spinel: A case for tetrahedrally coordinated Mn^{3+} in an oxygen-based structure. American Mineralogist, 92, 27–33.

Bosi, F., Agrosì, G., Lucchesi, S., Melchiorre, G., and Scandale, E. (2005a) Mn-tourmaline from island of Elba (Italy): Crystal chemistry. American Mineralogist, 90, 1661–1668.

Bosi, F., Andreozzi, G.B., Federico, M., Graziani, G., and Lucchesi, S. (2005b) Crystal chemistry of the elbaite-schorl series. American Mineralogist, 90, 1784–1792.

Bosi, F., Balić-Žunić, T., and Surour, A.A. (2010) Crystal structure analysis of four tourmalines from the Cleopatra's Mines (Egypt) and Jabal Zalm (Saudi Arabia), and the role of Al in the tourmaline group. American Mineralogist, 95, 510–518.

Bosi, F., Andreozzi, G.B., Skogby, H., Lussier, A., Ball, N.A., and Hawthorne, F.C. (2011) Fluor-elbaite, IMA 2011-071. CNMNC Newsletter No. 11, December 2011, p. 2891. Mineralogical Magazine, 75, 2887–2893.

Burns, P.C., MacDonald, D.J., and Hawthorne, F.C. (1994) The crystal-chemistry of manganese-bearing elbaite. Canadian Mineralogist, 32, 31–41.

Castañeda, C., Oliveira, E.F., Gomes, N., and Pedrosa-Soares, A.C. (2000) Infrared study of OH sites in tourmaline from the elbaite-schorl series. American Mineralogist, 85, 1503–1507.

Choi, J.B. and Grover, J. (2006) Synthesis and Rietveld structure refinement of Mn-tourmalines (Tsilaisite). Journal of the Mineralogical Society of Korea, 19, 15–29.

Duparc, L., Wunder, M., and Sabot, R. (1910) Les minéraux des pegmatites des environs d'Antsirabe à Madagascar. Mémoires de la Société de physique et d'Histoire Naturelle de Genève, 36, 283–410.

Ertl, A., Hughes, J.M., Prowatke, S., Rossman, G.R., London, D., and Fritz, E.A. (2003) Mn-rich tourmaline from Austria: structure, chemistry, optical spectra, and relations to synthetic solid solutions. American Mineralogist, 88, 1369–1376.

Ertl, A., Rossman, G.R., Hughes, J.M., London, D., Wang, Y., O'Leary, J.A., Dyar, M.D., Prowatke, S., Ludwig, T., and Tillmanns, E. (2010) Tourmaline of the elbaite-schorl series from the Himalaya Mine, Mesa Grande, California: A detailed investigation. American Mineralogist, 95, 24–40.

Federico, M., Andreozzi, G.B., Lucchesi, S., Graziani, G., and César-Mendes, J. (1998) Crystal chemistry of tourmalines. I. Chemistry, compositional variations and coupled substitutions in the pegmatite dikes of the Cruzeiro mine, Minas Gerais, Brazil. Canadian Mineralogist, 36, 415–431.

Foit, F.F. Jr. (1989) Crystal chemistry of alkali-deficient schorl and tourmaline structural relationships. American Mineralogist, 74, 422–431.

Gonzalez-Carreño, T., Fernandez, M., and Sanz, J. (1988) Infrared and electron microprobe analysis in tourmalines. Physics and Chemistry of Minerals, 15, 452–460.

Hawthorne, F.C. (1996) Structural mechanisms for light-element variations in tourmaline. Canadian Mineralogist, 34, 123–132.

——— (2002) Bond-valence constraints on the chemical composition of tourmaline. Canadian Mineralogist, 40, 789–797.

Hawthorne, F.C. and Henry, D. (1999) Classification of the minerals of the tourmaline group. European Journal of Mineralogy, 11, 201–215.

Henry, D.J. and Dutrow, B.L. (2011) The incorporation of fluorine in tourmaline: internal crystallographic controls or external environmental influences? Canadian Mineralogist, 49, 41–56.

Henry, D.J., Novák, M., Hawthorne, F.C., Ertl, A., Dutrow, B., Uher, P., and Pezzotta, F. (2011) Nomenclature of the tourmaline supergroup minerals. American Mineralogist, 96, 895–913.

Kunitz, W. (1929) Die Mischungsreihen in der Turmalingruppe und die genetischen Beziehungen zwischen Turmalinen und Glimmern. Chemie der Erde, 4, 208–251.

London, D. (2011) Experimental synthesis and stability of tourmaline: a historical perspective. Canadian Mineralogist, 49, 117–136.

Lussier, A.J., Aguiar, P.M., Michaelis, V.K., Kroeker, S., Herwig, S., Abdu, Y., and Hawthorne, F.C. (2008) Mushroom elbaite from the Kat Chay mine, Momeik, near Mogok, Myanmar: I. Crystal chemistry by SREF, EMPA, MAS NMR and Mössbauer spectroscopy. Mineralogical Magazine, 72, 747–761.

Lussier, A.J., Aguiar, P., Michaelis, V., Kroeker, S., and Hawthorne, F.C. (2009) The occurrence of tetrahedrally coordinated Al and B in tourmaline: An ^{11}B and ^{27}Al MAS NMR study. American Mineralogist, 94, 785–792.

Lussier, A.J., Hawthorne, F.C., Aguiar, P.M., Michaelis, V.K., and Kroeker, S. (2011a) Elbaite-liddicoatite from Black Rapids glacier, Alaska. Periodico di Mineralogia, 80, 57–73.

Lussier, A.J., Abdu, Y., Hawthorne, F.C., Michaelis, V.K., Aguiar, P.M., and Kroeker, S. (2011b) Oscillatory zoned liddicoatite from Anjanabonoina, central Madagascar. I. Crystal chemistry and structure by SREF and ^{11}B and ^{27}Al MAS NMR spectroscopy. Canadian Mineralogist, 49, 63–88.

Mandarino, J.A. (1976) The Gladstone-Dale relationship. Part I: derivation of new constants. Canadian Mineralogist, 14, 498–502.

——— (1981) The Gladstone-Dale relationship. Part IV: the compatibility concept and its application. Canadian Mineralogist, 19, 441–450.

Martínez-Alonso, S., Rustad, J.R., and Goetz, A.F.H. (2002) Ab initio quantum mechanical modeling of infrared vibrational frequencies of the OH group in dioctahedral phyllosilicates. Part II: Main physical factors governing the OH vibrations. American Mineralogist, 87, 1224–1234.

Novák, M., Povondra, P., and Selway, J.B. (2004) Schorl-oxy-schorl to dravite-oxy-dravite tourmaline from granitic pegmatites; examples from the Moldanubicum, Czech Republic. European Journal of Mineralogy, 16, 323–333.

Novák, M., Škoda, P., Filip, J., Macek, I., and Vaculovič, T. (2011) Compositional trends in tourmaline from intragranitic NYF pegmatites of the Tøebíč Pluton, Czech Republic; electron microprobe, Mössbauer and LA-ICP-MS study. Canadian Mineralogist, 49, 359–380.

Nuber, B. and Schmetzer, K. (1984) Structural refinement of tsilaisite (manganese tourmaline). Neues Jahrbuch für Mineralogie Monatshefte, 301–304.

Rossman, G.R. and Mattson, S.M. (1986) Yellow, Mn-rich elbaite with Mn–Ti intervalence charge transfer. American Mineralogist, 71, 599–602.

Sahama, T.G., Knorring, O., and Tornroos, R. (1979) On tourmaline. Lithos, 12, 109–114.

Schmetzer, K. and Bank, H. (1984) Crystal chemistry of tsilaisite (manganese tourmaline) from Zambia. Neues Jahrbuch für Mineralogie Monatshefte, 61–69.

Shabaga, B.M., Fayek, M., and Hawthorne, F.C. (2010) Boron and lithium isotopic compositions as provenance indicators of Cu-bearing tourmalines. Mineralogical Magazine, 74, 241–255.

Sheldrick, G.M. (2008) A short history of SHELX. Acta Crystallographica, A64, 112–122.

Shigley, J.E., Kane, R.E., and Manson, D.V. (1986) A notable Mn-rich gem elbaite tourmaline and its relationship to "tsilaisite". American Mineralogist, 71, 1214–1216.

Simmons, W.B., Falster, A.U., and Laurs, B.M. (2011) A survey of Mn-rich yellow tourmaline from worldwide localities and implications for the petrogenesis of the granitic pegmatites. Canadian Mineralogist, 49, 301–319.

Slivko, M.M. (1959) Manganese tourmalines. Mineralogiyeskii Sbornik (Mineralogical Magazine of the Geological Society of Lvov), 13, 139–148 (in Russian).

——— (1961) Manganese tourmalines. International Geology Review, 3, 195–201.

van Hinsberg, V.J. (2011) Preliminary experimental data on trace-element partitioning between tourmaline and silicate melt. Canadian Mineralogist, 49, 153–163.

van Hinsberg, V.J. and Schumacher, J.C. (2009) The geothermobarometric potential of tourmaline, based on experimental and natural data. American Mineralogist, 94, 761–770.

van Hinsberg, V.J., Henry, D.J., and Marschall, H.R. (2011) Tourmaline: an ideal indicator of its host environment. Canadian Mineralogist, 49, 1–16.

MANUSCRIPT RECEIVED OCTOBER 7, 2011
MANUSCRIPT ACCEPTED JANUARY 26, 2012
MANUSCRIPT HANDLED BY FERNANDO COLOMBO